Physics of the Earth and Planetary Interiors 262 (2017) 1–7

Contents lists available at ScienceDirect

Physics of the Earth and Planetary Interiors

journal homepage: www.elsevier.com/locate/pepi

Inversion of the moment-tensor M_{rr} components of the 2012 Sumatra strike-slip double earthquake using radial normal modes

Eliška Zábranová *, Ctirad Matyska

Department of Geophysics, Faculty of Mathematics and Physics, Charles University, V Holešovičkách 2, CZ-18000 Prague, Czech Republic

ARTICLE INFO

Article history:
Received 28 June 2016
Received in revised form 3 October 2016
Accepted 7 October 2016
Available online 15 October 2016

Keywords:
2012 Sumatra earthquakes
Superconducting-gravimeter data
Radial modes
CMT inversion

ABSTRACT

On April 11, 2012, two strike-slip Sumatra earthquakes with moment magnitudes higher than 8 generated strong, preferentially horizontal, motions. If only body and surface waves are inverted, their centroid-moment-tensor (CMT) parameters producing vertical motions, in particular the M_{rr} components, are poorly resolved. Independent constraints can be obtained from observations of the radial free-oscillation modes. The signal of radial modes is acquired from four unperturbed superconducting gravimeter records with low noise levels in submillihertz frequency range. We show that the observed signal substantially differs from the synthetic calculations for most of the published CMTs except for the Global CMT solution, which agrees better. We perform modal inversions considering uncertainties in centroid times and calculate marginal posterior probability density function of the M_{rr} components. The amplitude-spectrum inversion is robust enough to estimate the intervals of admissible M_{rr} values. Finally, we incorporate also a phase information and reduce the trade-off between the M_{rr} components of the two studied events.

1. Introduction

Two strike-slip earthquakes with moment magnitudes higher than 8 occurred off the west coast of the northern Sumatra on April 11, 2012, Fig. 1, where faults within the oceanic lithosphere of the Indo-Australia plate were activated. Tectonic explanation of such large unprecedented strike-slip intraplate earthquakes is rather complicated. Delescluse et al. (2012) suggest a continuing intraplate deformation between India and Australia, that followed the stress transfer after the Aceh 2004 and Nias 2005 megathrust earthquakes, on preexisting meridian-aligned fault planes of the oceanic lithosphere. Satriano et al. (2012) favor rupture jumping along reactivated NNE–SSW inherited faults that failed sequentially. Reactivation of these faults is also favoured by Andrade and Rajendran (2014). Other models argue that the earthquake pair ruptured two WNW–ESE oriented faults (Duputel et al., 2012;Yue et al., 2012). More complex rupture patterns with varying fault orientations have also been suggested (Meng et al., 2012;Zhang et al., 2012; Ishii et al., 2013;Wei et al., 2013).

Hayes (2012) and Shao et al. (2012) performed finite source inversions from broadband waveforms of P, SH and surface waves and favor a NNE–SSW primary nodal plane of the first, $M_w = 8.6$, event but the second option was not excluded. As to the centroid moment tensor (CMT), there are inconsistencies in routine agency solutions, see Table 1 (the first event) and 2 (the second event), respectively. One can see that the differences among these agency solutions are remarkable. These strike-slip earthquakes generated strong horizontal motions and the M_{rr} component contributes about only 10% to the scalar moment M_0. So, the inverted signal from the body and surface waves is less sensitive to the M_{rr} component than to the other moment tensor components. We assume the trace of the CMT to be zero, and thus only two diagonal components remain independent. The $M_{\phi\phi}$ components seem to be robust in the presented inversion and the question arises whether the remaining diagonal terms can be better constrained by an independent observation.

In this study we demonstrate that the observations of the radial free-oscillations can substantially improve the constraint on the diagonal CMT elements because the radial modes are generated only by the moment tensor component M_{rr}. However, the situation is complicated by the fact that the time difference between the events was only ~124 min and, therefore, we must deal with the M_{rr} components of both earthquakes simultaneously to explain the radial mode ${}_0S_0$ and ${}_1S_0$ oscillations observable for several weeks. It results in systematic trade-off that will be analyzed in detail.

* Corresponding author.
E-mail address: eliskazabranova@centrum.cz (E. Zábranová).

http://dx.doi.org/10.1016/j.pepi.2016.10.001
0031-9201/

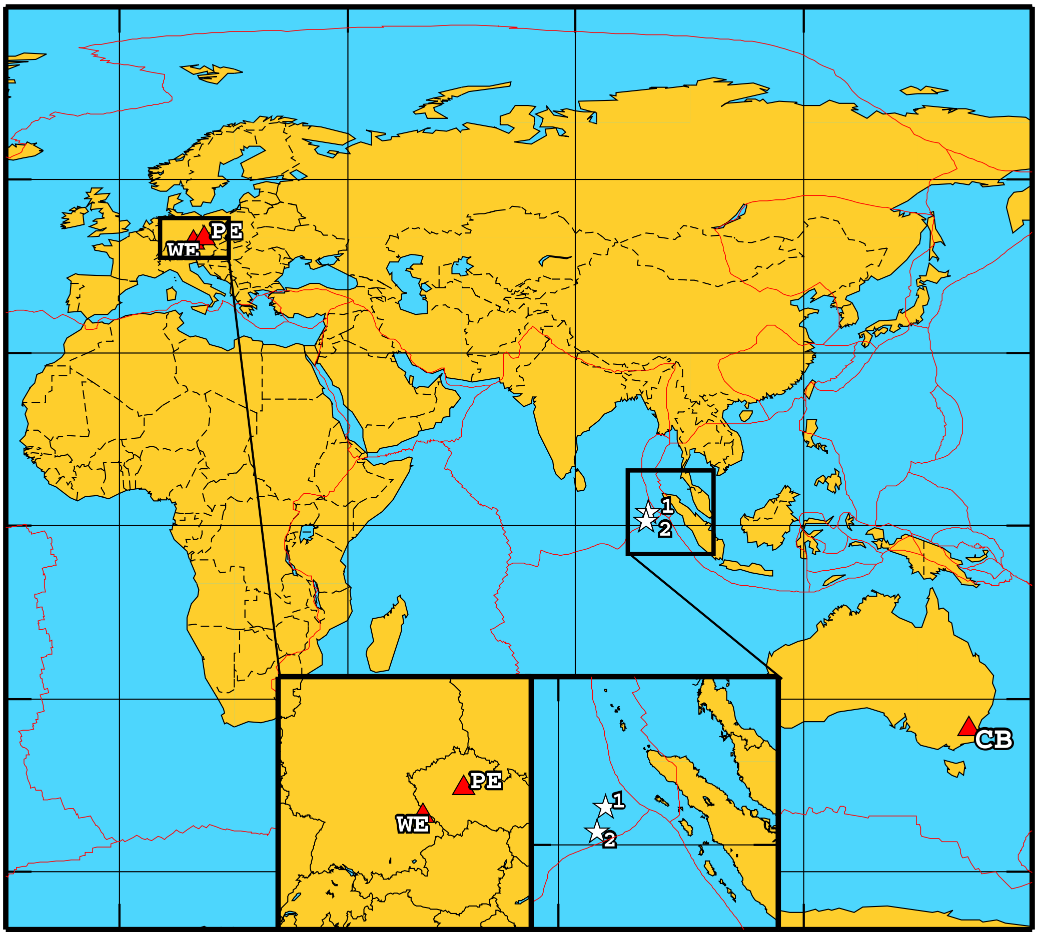

Fig. 1. Locations of the stations Pecný (PE), Canberra (CB) and Wettzell (WE) and epicentres of the two studied earthquakes. The plate boundaries were adopted from Bird (2003).

Table 1
M8.6: April 11, 2012 Sumatra earthquake agency solutions; Global CMT solution (PS1), USGS CMT solution (PS2), USGS Wphase solution (PS3). http://earthquake.usgs.gov/archive/product/phase-data/usp000jhh2/us/1415324847888/quakeml.xml http://www.emsc-csem.org/Earthquake/mtfull.php?id=261636.

	Latitude	Longitude	Depth [km]	Centroid time	M_0 [10^{21} Nm]
PS1	2.24 N	92.78E	40.0	08:39:29.8	9.0
PS2	2.24 N	93.10E	40.0	08:39:32.6	8.5
PS3	2.25 N	92.87E	25.0		9.0

[10^{21} Nm]	M_{rr}	$M_{\theta\theta}$	$M_{\phi\phi}$	$M_{r\theta}$	$M_{r\phi}$	$M_{\theta\phi}$
PS1	1.36	−5.91	4.55	−3.96	0.46	−6.15
PS2	0.40	−5.39	4.98	1.74	−1.57	−6.31
PS3	1.25	−5.99	4.74	1.34	−0.63	−7.03

Table 2
M8.2: April 11, 2012 Sumatra earthquake agency solutions; Global CMT solution (PS1*), USGS CMT solution (PS2*), USGS Wphase solution (PS3*). http://earthquake.usgs.gov/archive/product/phase-data/usp000jhjb/us/1415324848136/quakeml.xml http://www.emsc-csem.org/Earthquake/mtfull.php?id=261684.

	Latitude	Longitude	Depth [km]	Centroid time	M_0 [10^{21} Nm]
PS1*	0.76 N	92.25E	53.7	10:43:37.4	2.5
PS2*	0.92 N	92.49E	43.0	10:43:50.3	2.2
PS3*	0.77 N	92.45E	16.0		3.9

[10^{21} Nm]	M_{rr}	$M_{\theta\theta}$	$M_{\phi\phi}$	$M_{r\theta}$	$M_{r\phi}$	$M_{\theta\phi}$
PS1*	0.59	−1.67	1.08	−1.08	−0.46	−1.89
PS2*	0.45	−1.30	0.85	0.21	−0.84	−1.63
PS3*	−1.18	0.18	1.00	−0.92	−1.33	−3.38